Proceedings of DETC'01
2001 ASME Design Engineering Technical Conferences
September 9-12, 2001, Pittsburgh, Pennsylvania, USA

DETC2001/DAC-21026

WORKSPACE-BASED DESIGN OF PARALLEL MANIPULATORS OF STAR TOPOLOGY WITH A GENETIC ALGORITHM

Luc Baron
Department of Mechanical Engineering
Ecole Polytechnique de Montréal
C.P. 6079, succ. CV, Montréal, QC, Canada H3C 3A7
Email: baron@meca.polymtl.ca
http://www.meca.polymtl.ca/profs/baron

ABSTRACT

This paper presents the results of the implementation of a genetic algorithm for the design of parallel manipulators of Star topology based on the characteristics of its workspace (W). The algorithm allows to propose new geometries of manipulators that maximize the weighted sum of the volume of W, the percentage of W having a dexterity index greater than a minimum threshold, and a shape ration of W. The algorithm has proven to be effective by proposing a new design that overcomes, by a factor of 3.636, the performances of the original Y Star design, after evaluating the performances of only 2000 alternative designs, which correspond to a traveling of only 2.02×10^{-16}% through the search space of this design problem.

NOMENCLATURE

A, B Frames attached to body A and B.
A_i, A'_i Displacement limits of leg i along the screw axis i.
B_i, B'_i Attachment points of leg i on body B, i.e., the EE.
E_i, E'_i Attachment points of leg i along the screw axis i.
$\mathbf{p}$ Position vector of the origin of B in A.
$\mathbf{a}_i$ Position vector of A_i in A.
$\mathbf{b}_i$ Position vector of B_i in B.
$\mathbf{e}_i$ Unit vector along the screw axis i.
$\mathbf{f}_i$ Unit vector from E_i toward B'_i in A.
$\mathbf{m}_i$ Position vector of B'_i relative to E_i in A.
q_i Controlled and measured displacement of E_i along $\mathbf{e}_i$.
l_i Leg length between points E_i and B'_i.

INTRODUCTION

In general, parallel manipulators are particularly interesting because they possess complementary characteristics to serial ones. In fact, the formers can be used in situations where characteristics of the latter cannot satisfy the application requirements. It is noteworthy that parallel manipulators possess a higher load carrying capacity, a better positioning accuracy or speed, but also a lower workspace volume, more singularity problems and an increased complexity when solving the direct kinematic problem compared to serial manipulators of equivalent size (Baron and Angeles, 2000). The design of parallel manipulators is a complex activity involving many technical and creative behaviors. The designer must evaluate the capacity of each potential design to meet the application requirements. Among others, the manipulator mobility, stiffness, singularity and dexterity are posture dependent ratings, and hence, require to be evaluated a set of postures within the manipulator workspace. Unfortunately, these ratings are usually available only in an algorithmic form or as a non-derivable equation, and thus, standard optimization methods based on the gradient cannot be used to reach the specifications. The designer must use evaluation programs in order to measure the performances of each potential design and then determined the geometrical modifications that would improve the performances of these designs. This iterative process is extremely long and tedious since it is based only on the designer's intuition and experiences. Genetic algorithms (GAs) are powerful stochastic optimization techniques (Goldberg, 1989) and are considered here for that purpose.

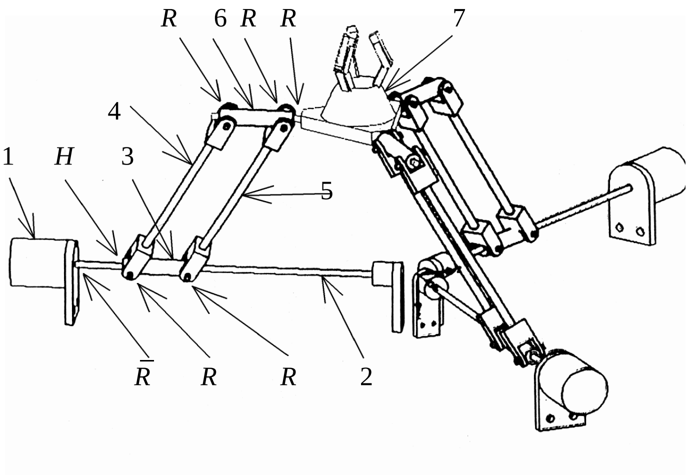

Figure 1. THE Y-STAR PARALLEL MANIPULATOR

PROBLEM FORMULATION

The kinematics of robotic manipulators can be described with the concept of *kinematic chain*, which carries both topological and geometrical informations. A kinematic chain is defined as a mechanical system in which rigid bodies, called *links*, are coupled by *lower kinematic pairs*. There are six of such pairs, namely, revolute (*R*), prismatic (*P*), cylindrical (*C*), helicoidale (*H*), planar (*E*), and spherical (*S*). The *topology* refers to the layout of these pairs along the chain, while the *geometry* refers to the relative location of the pairs on each link. As shown in Fig.1, the kinematic chain of the Y-Star parallel manipulator (Hervé, 1991) is composed of three serial chains acting in parallel, i.e., an actuated *R* joint—denoted $\bar{R}$—connecting link 1 to link 2, a passive *H* joint connecting link 2 to 3, two passive *R* joints connecting link 3 to links 4 and 5, two passive *R* joints connecting links 4 and 5 to link 6, and a passive *R* joint connecting link 6 to link 7.

In order to maintain the translational three-degree-of-freedom mobility of the EE, the four *R* joint axes of the closed loops formed by links 3 to 6 must always be parallel, while the axis of the *R* joint connecting each leg to the EE must be parallel to its corresponding *H* worm screw axis. All the other relative positions and orientations of the kinematic pairs on the different links of the parallel manipulators of this topology can be general, and hence, be described with geometrical parameters. Although being restrictive, the following assumption is made in order to limit the dimension of the search space.

Assumption: The three worm screw axes intersect at a point.

This simplification assumption allows to remove the few geometric parameters that would be required to describe three none intersecting axes. This limit to the scope of possible designs appears reasonable to the author's knowledge.

GEOMETRIC PARAMETERS

As shown in Fig.2, frames $\mathcal{A}$ and $\mathcal{B}$ are attached to the base and the EE, which are denoted *A* and *B*, respectively. Without lost of generality, the origin of frame $\mathcal{A}$ is located at the intersection point of three worm screw axes, the *x*-axis aligned along the worm screw 1. The orientation of the three axes is described with three geometric parameters, i.e., γ_2, ω_2, γ_3 and ω_3, and thus, the unit vector $\mathbf{e}_i$ along each worm screw axis *i* is given as

$$\mathbf{e}_1 = \begin{bmatrix} 1 \\ 0 \\ 0 \end{bmatrix}, \quad \mathbf{e}_2 = \begin{bmatrix} \cos\gamma_2 \\ \sin\gamma_2 \sin\omega_2 \\ \sin\gamma_2 \cos\omega_2 \end{bmatrix}, \quad \mathbf{e}_3 = \begin{bmatrix} \cos\gamma_3 \\ \sin\gamma_3 \sin\omega_3 \\ \sin\gamma_3 \cos\omega_3 \end{bmatrix} \quad (1)$$

The controlled joint variable, namely q_i, allows the displacement of points E_i and E'_i of Link 3 along the worm screw axis $\mathbf{e}_i$ between the limits defined by points A_i and A'_i. These last two points are located along $\mathbf{e}_i$ at a distance v_i and u_i from the origin, i.e,

$$\mathbf{a}_i = v_i \mathbf{e}_i, \quad \mathbf{a}'_i = u_i \mathbf{e}_i, \quad i = 1,2,3. \quad (2)$$

while the distance between E_i and E'_i is defined as e_i. For the sake of removing designs that differs only from a scale factor, v_1 is arbitrarily set to 150 units of length, namely *u*, and consequently, any further lengths will be expressed with this unit *u*. The geometry of the EE is defined at the home position of the controlled joints, i.e., $q_1 = q_2 = q_3 = 0$, as the position in $\mathcal{A}$ of three points of general coordinates, i.e.,

$$[\mathbf{b}_1]_A = \begin{bmatrix} x_1 \\ y_1 \\ z_1 \end{bmatrix}, \quad [\mathbf{b}_2]_A = \begin{bmatrix} x_2 \\ y_2 \\ z_2 \end{bmatrix}, \quad [\mathbf{b}_3]_A = \begin{bmatrix} x_3 \\ y_3 \\ z_3 \end{bmatrix} \quad (3)$$

Again here, for the sake of removing designs that differs only from a scale factor of the EE relative to the base, we arbitrarily set z_1 to 50 *u*. Finally, the total number of geometric parameters of this design problem is 20, i.e., γ_2, ω_2, v_2, x_1, y_1, x_2, y_2, ω_3, v_3, e_1, z_2, x_3, y_3, z_3, e_2, e_3, u_1, u_2, u_3 and γ_3.

KINEMATIC MODEL

Each leg of the manipulator forms a kinematic loop passing through the origin of frames $\mathcal{A}$ and $\mathcal{B}$ and points A_i, E_i, B'_i and B_i. The closure equation of each loop is written as

$$\mathbf{m}_i = \mathbf{z}_i + q_i \mathbf{e}_i, \quad i = 1,2,3, \quad (4)$$

where vector $\mathbf{z}_i$ is defined as

$$\mathbf{z}_i \equiv \mathbf{p} + \mathbf{b}_i + e_i \mathbf{e}_i - \mathbf{a}_i. \quad (5)$$

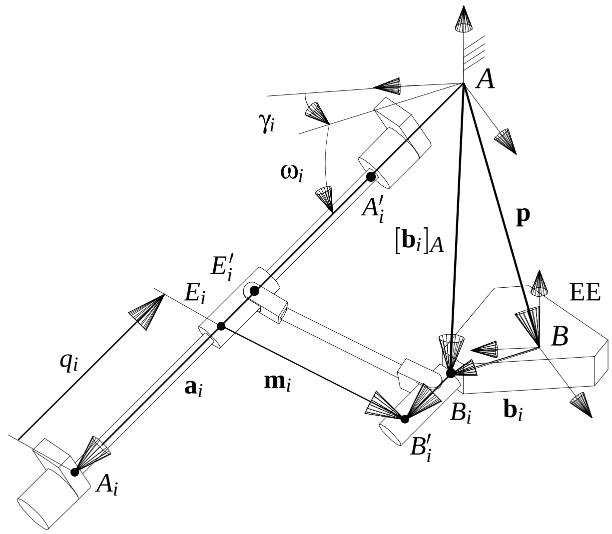

Figure 2. LEG GEOMETRY OF THE STAR TOPOLOGY

For a given manipulator geometry, the length of each leg, denoted l_i, is a known constant, and hence, the inverse kinematics of these manipulators can be written as

$$\| \mathbf{m}_i \|^2 = \mathbf{m}_i^T \mathbf{m}_i = l_i^2, \quad i = 1,2,3. \tag{6}$$

Upon substituting eq.(4) into (6) yields the following quadratic polynomial in q_i, i.e.,

$$q_i^2 + 2\mathbf{z}_i^T \mathbf{e}_i q_i + \mathbf{z}_i^T \mathbf{z}_i - l_i^2 = 0, \tag{7}$$

where the two solutions of q_i for each leg can be computed as

$$q_i = -\mathbf{z}_i^T \mathbf{e}_i \pm \sqrt{\mathbf{z}_i^T \mathbf{e}_i \mathbf{z}_i^T \mathbf{e}_i - \mathbf{z}_i^T \mathbf{z}_i + l_i^2} \tag{8}$$

The inverse kinematics of manipulators of this class can have up to $2^3 = 8$ combinations of solutions of joint positions $\{q_i\}_1^3$ for the same EE position. Upon derivation of the eq.(7) with respect to time yields following velocity relationship, i.e.,

$$\mathbf{A}\dot{\mathbf{p}} = \mathbf{B}\dot{\mathbf{q}}, \quad \dot{\mathbf{q}} \equiv [\dot{\mathbf{q}}_1 \; \dot{\mathbf{q}}_2 \; \dot{\mathbf{q}}_3]^{\mathbf{T}}, \tag{9}$$

where $\dot{\mathbf{p}}$ is the velocity vector of the origin of B in A (or the EE) and $\dot{\mathbf{q}}$ the joint velocity vector of the manipulator. Moreover, **A** and **B** are, respectively, the parallel and serial Jacobian matrices of the manipulator at hand, i.e.,

$$\mathbf{A} = \begin{bmatrix} \mathbf{m}_1^T \\ \mathbf{m}_2^T \\ \mathbf{m}_3^T \end{bmatrix}, \quad \mathbf{B} = \begin{bmatrix} b_1 & 0 & 0 \\ 0 & b_2 & 0 \\ 0 & 0 & b_3 \end{bmatrix}, \tag{10}$$

where $b_i \equiv -\mathbf{m}_i^T \mathbf{e}_i$.

GENETIC ALGORITHM

GAs are powerful stochastic optimization techniques based on the analogy of the mechanics of natural genetics, and imitates the Darwinian survival-of-the-fittest approach. The method uses bits of string as the *genotype* to represent the numerical values of the geometric parameters, called in this context *phenotype*, of a potential design. The coding of the phenotype, denoted p_i into the genotype, denoted g_i requires the discretization of p_i between the limits $p_{i_{min}}$ and $p_{i_{max}}$ with a chosen resolution, denoted r_i, in order to obtain the corresponding genotype $g_i \in [g_{i_{min}}, g_{i_{min}} + r_i, \cdots, g_{i_{max}}]$ as

$$g_i = f(p_i), \quad p_{i_{min}} \le p_i \le p_{i_{max}}, \tag{11}$$

where $f(p_i)$ produces an integer computed as

$$f(p_i) \equiv \text{round}(\frac{p_i - p_{i_{min}}}{r_i}) + g_{i_{min}} \tag{12}$$

with r_i defined as

$$r_i \equiv \frac{(p_{i_{max}} - p_{i_{min}})}{(g_{i_{max}} - g_{i_{min}})} \tag{13}$$

Alternatively, the decoding of g_i into p_i is performed with

$$p_i = f^{-1}(g_i), \quad g_i \in [g_{i_{min}}, g_{i_{min}} + r_i, \cdots, g_{i_{max}}], \tag{14}$$

where $f^{-1}(g_i)$ is defined as

$$f^{-1}(g_i) \equiv r_i(g_i - g_{i_{min}}) + p_{i_{min}} \tag{15}$$

As shown in Table 1, the phenotypes of this design problem require a total of 88 bits, and for the sake of computer handling facility three 32-bits variables (96 bits) is used as follows

$$G_p = \left\{ \begin{array}{l} \underbrace{1001}_{g_1}\underbrace{1100}_{g_2}\underbrace{0001}_{g_3}\underbrace{10011}_{g_4}\underbrace{11001}_{g_5}\underbrace{11011}_{g_6}\underbrace{10010}_{g_7} \\ \underbrace{1111}_{g_8}\underbrace{0011}_{g_9}\underbrace{0101}_{g_{10}}\underbrace{11110}_{g_{11}}\underbrace{11001}_{g_{12}}\underbrace{01011}_{g_{13}}\underbrace{01001}_{g_{14}} \\ \underbrace{0111}_{g_{15}}\underbrace{1001}_{g_{16}}\underbrace{0101}_{g_{17}}\underbrace{1110}_{g_{18}}\underbrace{0101}_{g_{19}}\underbrace{0011}_{g_{20}}10001111 \end{array} \right\}$$

Table 1. CODING AND DECODING OF THE PHENOTYPES

Parameters		$p_{i_{min}}$	$p_{i_{max}}$	r_i	units	g_i	$g_{i_{min}}$	$g_{i_{max}}$
p_1	γ_2	15	165	15	deg	g_1	0	10
p_2	ω_2	-90	90	15	deg	g_2	0	12
p_3	v_2	0	150	15	u	g_3	0	10
p_4	x_1	-100	100	10	u	g_4	0	20
p_5	y_1	-100	100	10	u	g_5	0	20
p_6	x_2	-100	100	10	u	g_6	0	20
p_7	y_2	-100	100	10	u	g_7	0	20
p_8	ω_3	-90	90	15	deg	g_8	0	12
p_9	v_3	0	150	15	u	g_9	0	10
p_{10}	e_1	0	120	15	u	g_{10}	0	8
p_{11}	z_2	-100	100	10	u	g_{11}	0	20
p_{12}	x_3	-100	100	10	u	g_{12}	0	20
p_{13}	y_3	-100	100	10	u	g_{13}	0	20
p_{14}	z_3	-100	100	10	u	g_{14}	0	20
p_{15}	e_2	0	120	15	u	g_{15}	0	8
p_{16}	e_3	0	120	15	u	g_{16}	0	8
p_{17}	u_1	0	50	5	u	g_{17}	0	10
p_{18}	u_2	0	50	5	u	g_{18}	0	10
p_{19}	u_3	0	50	5	u	g_{19}	0	10
p_{20}	γ_3	180	345	15	deg	g_{20}	0	12

The GA uses iterative improvement of a population of potential designs by mean of three basic operations: *reproduction*, *evaluation* and *natural selection*.

Reproduction: Based on an *elitist strategy*, the characteristics of the most promising designs are recombined by *crossover* and *mutation* in order to create new designs. As shown in Fig.3, the crossover operation is formed by inverting the end part of the genotype of two fellow designs at a randomly selected crossover site. The mutation is the inversion of a bit during the crossover operation.
Evaluation: The performances of each new design are measured along three indexes, while a weighted linear combination of the three former is the fourth index.
Natural selection: The fellow and new designs are classified along the four indexes, and only the best designs of each index are kept for the next generation.

In this work, the first generation start with 100 designs, 100 new designs are obtained by reproduction, and the best 25 none-identical designs of the four indexes are kept for the next generation. The probability of mutation must be lower than 5% in order

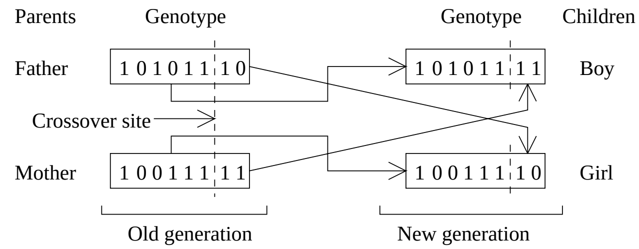

Figure 3. THE SIMPLE CROSSOVER OPERATION

to let the population mainly improve itself by crossover. The mutation produces movement in any direction, and thus, allows the possibility of jumping out of a local optimum and potentially found a more promising design.

WORKSPACE-BASED DESIGN

All our performance indexes are based directly or indirectly on the manipulator's workspace, denoted W, and hence, requires its determination. For this purpose, the *box method* (Merlet, 1997) is used, and for which a short summary appear below.

An initial box sufficiently large to completely contain W is chosen. This box is divided in 8 sub-boxes The corners of each box are verify with eq.(8) in order to produce solutions of q_i within the joint limits, and for which 3 cases may arise: completely included (black), partially included (grey), or totally outside of W (white). The first box (alway grey if properly chosen) and all other grey boxes are repeatedly subdivided and analyzed up to d times, a predefined depth. As a result, W is efficiently represented in the computer as an *octree*. For example, the workspace W (the black boxes) of the 4×4 array shown in Fig.4 can be represented with a *quadtree* (a concept equivalent to octree in 2D).

Unfortunately, this method can not distinguish between boxes coming from different *assembly modes*, and hence can pro-

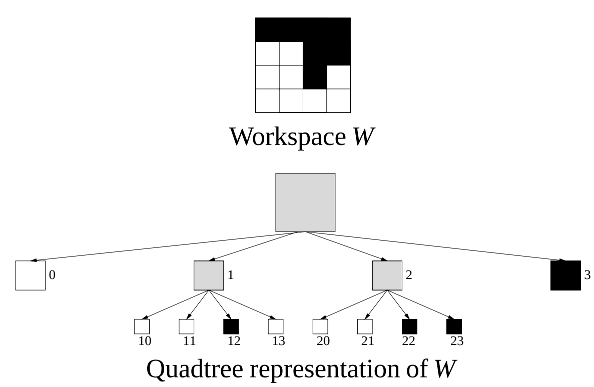

Figure 4. WORKSPACE AND ITS QUADTREE REPRESENTATION

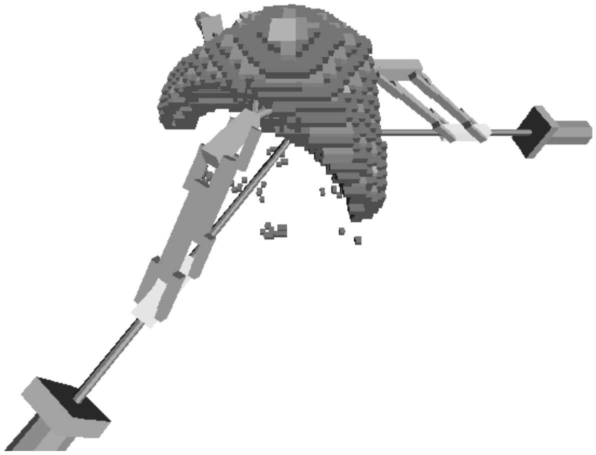

(a) 1^{st} assembly mode

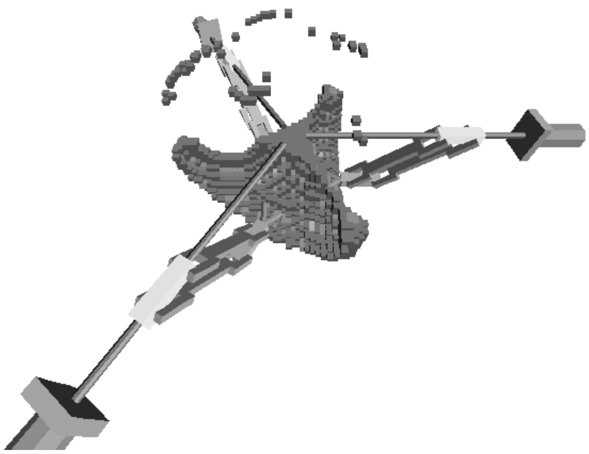

(b) 2^{nd} assembly mode

Figure 5. THE 2 ASSEMBLY MODES OF PARALLEL MANIPULATORS OF STAR TOPOLOGY

duce completely wrong results as it is the case in Tremblay and Baron (1999). It is recalled that a parallel manipulator can not move its end-effector from an assembly mode to another without disassembling the manipulator. Therefore, the workspace W must contain only boxes of the same assembly mode. This distinction can intuitively be done for Stewart-Gough platforms or the Y Star parallel manipulator (see Fig5), since their geometries are known. However in this work, the geometry is generalized and unknown, and consequently, the assembly mode becomes intuitively unpredictable. For this purpose, the mathematical concept of *aspect* (Chablat, 1998) is used to distinguish between portions of assembly modes that correspond to different *operational modes*. The limits between two aspects are defined as singularities of the serial Jacobian matrix. For example, the 8 aspects (or operational modes) of the first assembly mode of the Y Star parallel manipulator are shown in Fig.6.

Our three performance indexes are, respectively, the volume of W, denoted v_w, the shape ratio of W, denoted ρ_s, and the dexterity ratio, denoted ρ_d. The first index v_w is easily computed as the total number of smallest boxes totally included in W. The second index ρ_s is defined as the ratio of the volume of the largest cube completely inscribed in W over the volume of the smallest cube completely containing W. Finally, the third index is defined as the percentage of smallest boxes of W having a dexterity index greater than a minimum threshold of 0.25, where the dexterity index (Salisbury, 1982) of is computed as the ratio the minimum over the maximum singular values of the combined Jacobian matrix, i.e., $\mathbf{J} = \mathbf{B}^{-1}\mathbf{A}$. Thus, boxes with a dexterity index of zero and one mean singular and isotropic boxes, respectively. Moreover, a dexterity ratio of 0.5, for example, means 50% of W have a dexterity index greater than 0.25, which is a very interesting property, because manipulators exhibit their best kinematic performances at high dexterity indexes. The fourth performance index, denoted ρ, is defined as a weighted sum of the first three indexes so that the performance index of the Y Star produces an equal weight between the three indexes, and hence, we have

$$\rho = k_1 v_W + k_2 \rho_s + k_3 \rho_d, \tag{16}$$

where k_1, k_2 and k_3 are defined as $k_1 = 1.179 \times 10^{-6}\ u^{-3}$, $k_2 = 1.996$ and $k_3 = 0.555$, so that $\rho = 0.333 + 0.333 + 0.333 = 1.000$ for the Y Star parallel manipulator.

DESIGN RESULTS

The number of discrete values of each genotype g_i is given as $(g_{i_{max}} - g_{i_{min}} + 1)$, and hence, the total number of possible solutions of this design problem is computed as

$$\prod_{i=1}^{20} (g_{i_{max}} - g_{i_{min}} + 1) = 9.9 \times 10^{22} \tag{17}$$

Considering an average computing time for of each design of 21 sec. on a Pentium-II at 300 MHz, it would require 3.1×10^{15} years to compute the performances of all possible designs of this search space. Obviously, such a computation is unfeasible, and only approximative solutions to this design problem are seek. Table 2 and 3 show, respectively, the geometric parameters and the performance indexes of three expert designs found after only 20 generations relative to those of the Y Star design. These solutions have required the evaluation 2000 designs, which correspond to a traveling of only 2.02×10^{-16}% through the search space.

The three expert designs, shown in Fig.7, has been found with three different runs of our GA-based synthesis program from which the design having the best weighted sum ρ is selected. The experts #1 and #2 have been found from the same

Table 2. GEOMETRY OF THE THREE EXPERTS

Parameters		#1	#2	#3	Y Star	units
p_1	γ_2	15	15	75	120	deg
p_2	ω_2	-60	-60	0	0	deg
p_3	v_2	150	150	150	150	u
p_4	x_1	-20	-50	-10	40	u
p_5	y_1	-50	-70	-20	0	u
p_6	x_2	20	0	-20	-20	u
p_7	y_2	-80	-70	-30	40	u
p_8	ω_3	0	0	-75	0	deg
p_9	v_3	150	150	150	150	u
p_{10}	e_1	30	75	0	30	u
p_{11}	z_2	50	-10	80	50	u
p_{12}	x_3	70	-30	70	-20	u
p_{13}	y_3	-40	-20	80	-40	u
p_{14}	z_3	100	50	-60	50	u
p_{15}	e_2	15	15	15	30	u
p_{16}	e_3	30	30	30	30	u
p_{17}	u_1	15	20	20	10	u
p_{18}	u_2	30	10	20	10	u
p_{19}	u_3	40	10	45	10	u
p_{20}	γ_3	255	315	240	240	deg

initial and randomly generated population, but the crossover and mutation operations are randomly different, and converge differently toward slightly different designs. Alternatively, expert #3 has been found from a randomly different initial population, and has converged toward different designs. It is noteworthy that for all three runs, the population of designs after only 20 generations includes designs having performance indexes three times greater than those of the Y Star design. Moreover, our synthesis program proposes symmetric designs having a relative orientation of three worm screws at, or close to, 90 deg. A result that corroborates the research works on isotropic serial manipulators. Expert #2 has a higher ρ_d than expert #1, but also a slightly smaller v_W. However, expert #3 has a higher v_W than any others, a better ρ_s than the Y Star, but also a lower ρ_d. The latter being not really a disadvantage, since the dextrous volume, denoted v_d, can be computed as $v_d = \rho_d v_W$, where $v_d = 830286\ u^3$ for expert #3 and $v_d = 173140\ u^3$ for the Y Star. Although ρ_d of expert #3 is lower than the one of the Y Star, its dextrous volume v_d is almost 5 times larger than the corresponding volume of the Y Star. Clearly, expert #3 overcomes all the three indexes of the Y Star, and is globally 3.636 times better than the Y Star.

CONCLUSION

Our genetic algorithm has proven to be a very effective design tool for proposing new geometries of parallel manipulators of Star topology that maximize some characteristics of its workspace. The concepts of assembly and operational modes allowed the algorithm to compute performance indexes on only portions of W that are either free of parallel singularities or free of both parallel and serial singularities, respectively. The main result of the paper lies in the proposition of a new design that overcomes the performance indexes of the original Y Star design. This design, called for instance the *Expert Star* is further shown in Fig. 8 under a translational motion of its triangular end-effector. This design is globally 3.636 times better than the Y Star design. In the future, we intend to remove the assumption of three worm screw axes intersecting at a point and takes into account links obstruction in the computation of the workspace. Obviously, this will result in a significant increase in the size of the search space.

ACKNOWLEDGMENT

The author acknowledge the financial support of NSERC (National Sciences and Engineering Research Council of Canada) under grant OGPIN-203618 and FCAR (Fond Concerté d'aide à la Recherche of Quebec) under grant NC-66861.

REFERENCES

Baron, L. and Angeles, J., "The Direct Kinematics of Parallel Manipulators Under Joint-Sensor Redundancy", *IEEE Trans. on Robotics and Automation*, Vol. 16, No. 1, pp. 12–19, 2000.

Goldberg, D.E., *Genetic Algorithms in Search, Optimization, and Machine Learning*, Addison-Wesley, 412 pages, 1989.

Hervé, J.M., "Dispositif pour le déplacement en translation spaciale d'un élément dans l'espace, en particulier pour robot mécanique", *French Patent No. 9100286*, January 1991, *European Patent No. 91403521.7*, December 1991.

Merlet, J.-P., "Estimation efficace des caractéristiques de robots parallèles: Extremums des raideurs et coordonnées, vitesses, forces articulaires et Singularités dans un espace de travail en translation", *INRIA report*, 46 pages, 1997.

Tremblay, A. and Baron, L., "Geometrical Synthesis of Parallel Manipulators of Star-Like Topology with a Genetic Algorithm", *Proc. IEEE Int. Conf. on Robotics and Automation*, pp. 2446-2451, Detroit, USA, May 1999.

Chablat, D., "Domaines d'unicité et parcourabilité pour les manipulateurs pleinement parallèles", *Ph.D. These*, Université de Nantes, 182 pages, 1998.

Salisbury, J.-K. and Craig, J.-J., "Articulated Hands: Force Control and Kinematic Issues", *The Int. J. of Robotics Research*, Vol. 1, No. 1, pp. 4–17, 1982.

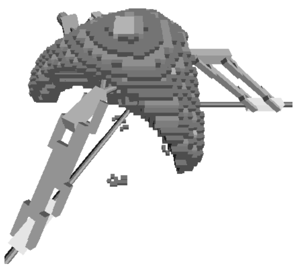

(a) 1^{st} mode

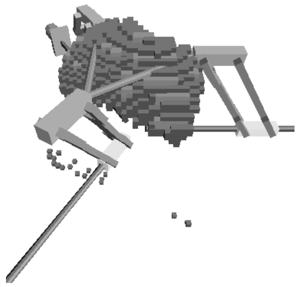

(b) 2^{nd} mode

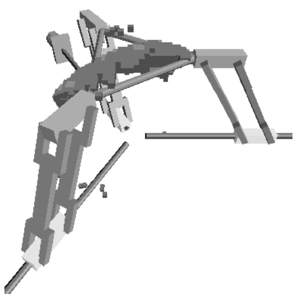

(c) 3^{rd} mode

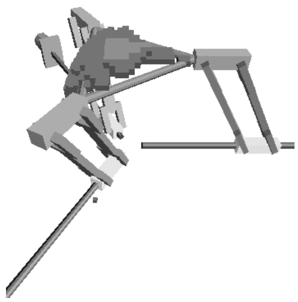

(d) 4^{th} mode

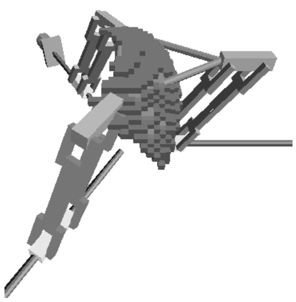

(e) 5^{th} mode

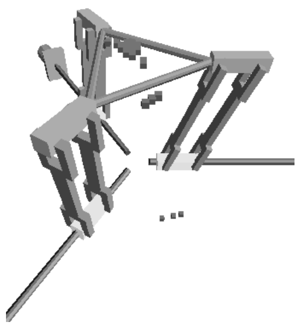

(f) 6^{th} mode

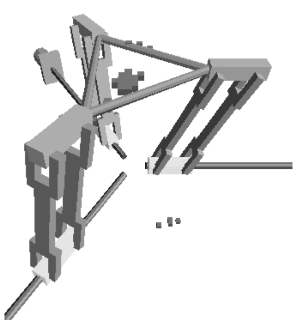

(g) 7^{th} mode

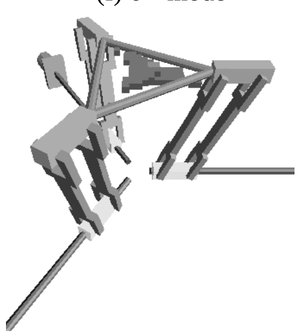

(h) 8^{th} mode

Figure 6. THE 8 OPERATIONAL MODES OF THE 1^{st} ASSEMBLY MODE OF THE Y STAR PARALLEL MANIPULATOR

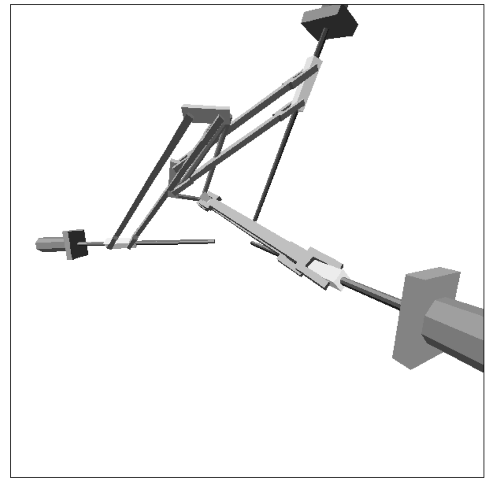

(a) Expert #1 (AG1)

(b) Expert #2

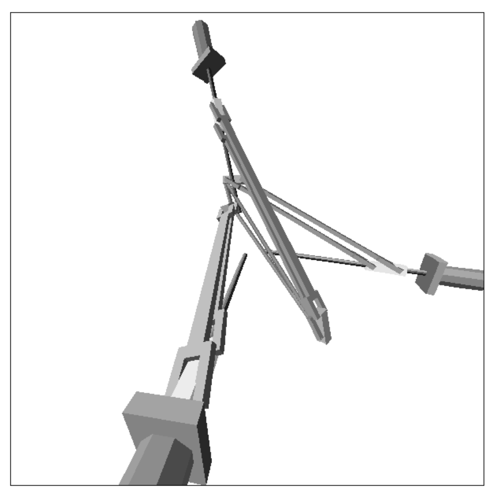

(c) Expert #3 (AG3)

Figure 7. THE THREE EXPERT MANIPULATORS

Table 3. PERFORMANCES OF THE THREE EXPERTS

Design	v_W	ρ_d	ρ_s	ρ
expert #1	1890625	0.674	0.414	3.422
expert #2	1857178	0.902	0.414	3.504
expert #3	2281006	0.364	0.375	3.636
Y Star	288086	0.601	0.167	1.000
units	u^3	none	none	none

(a) $\mathbf{p} = (-87.5,\ 23.2,\ -81.1)$

(b) $\mathbf{p} = (-38.3,\ 10,\ -65.5)$

(c) $\mathbf{p} = (-61.1,\ 10,\ -0.7)$

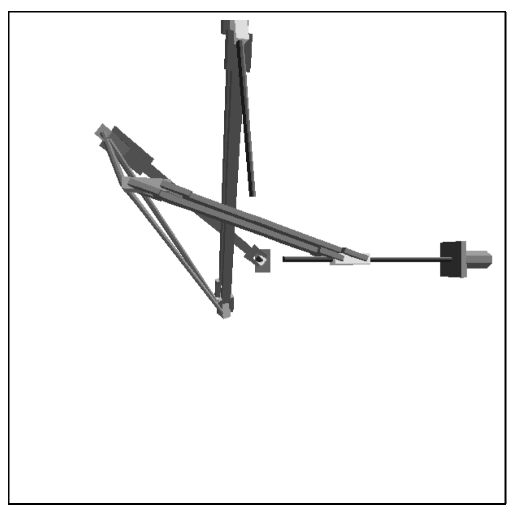

(d) $\mathbf{p} = (-68.3,\ 32.8,\ 23.3)$

Figure 8. MOTION OF THE EXPERT STAR